

On demand generation of propagation invariant photons with orbital angular momentum

Y. Jerónimo-Moreno, R. Jáuregui¹

¹*Instituto de Física, Universidad Nacional Autónoma de México,
Apartado Postal 20-364, México D. F. 01000, México**

We study the generation of propagation invariant photons with orbital angular momentum by spontaneous parametric down conversion (SPDC) using a Bessel-Gauss pump beam. The angular and conditional angular spectra are calculated for an uniaxial crystal optimized for type I SPDC with standard Gaussian pump beams. It is shown that, as the mean value of the magnitude of the transverse wave vector of the pump beam increases, the emission cone is deformed into two non coaxial cones that touch each other along a line determined by the orientation of the optical axis of the nonlinear crystal. At this location, the conditional spectrum becomes maximal for a pair of photons, one of which is best described by a Gaussian-like photon with a very small transverse wave vector, and the other a Bessel-Gauss photon with a distribution of transverse wave vectors similar in amplitude to that of the incident pump beam. A detailed analysis is then performed of the angular momentum content of SPDC photons by the evaluation of the corresponding transition amplitudes. As a result, we obtain conditions for the generation of heralded single photons which are approximately propagation invariant and have orbital angular momentum. A discussion is given about the difficulties in the interpretation of the results in terms of conservation of optical orbital angular momentum along the vector normal to the crystal surface. The angular spectra and the conditional angular spectra are successfully compared with available experimental data recently reported in the literature.

PACS numbers: 42.50.-p, 42.65.Lm

* rocio@fisica.unam.mx

I. INTRODUCTION

In the last two decades there has been huge advances in the generation of structured light beams with several spatial and dynamical features. Probably the best known examples correspond to beams with orbital angular momentum (OAM), e. g. Laguerre[1] and Bessel beams[2], though other possibilities with diverse transverse[3, 4] and longitudinal structure[5] are not less interesting. The richness of structured beams is inherited to several optical phenomena. Here we shall focus on spontaneous parametric down conversion (SPDC).

SPDC from structured beams can be useful for the implementation of quantum information protocols for which the encoding variables may be different from polarization, linear momentum or frequency of the photons. In quantum optics, two-photon states entangled in polarization, usually generated via a SPDC process, have become the most widely used entangled systems. In this case, the two photons in a pair usually have one of two orthogonal polarization directions [6]. In most cases, the description of the system is made in a Hilbert space of just two-dimensions, though the role of the other degrees of freedom of the photon should not be ignored in general. Quantum-enhanced technologies demand systems consisting of multiple entangled states, as well as quantum states entangled in multiple dimensions. The latter may, for instance, improve the communication channel efficiency in quantum cryptography [7]. The generation of two-photon states with multi-dimensional entanglement has been shown to be feasible, and the challenge to control it is the main subject of many theoretical and experimental current studies.

One way to produce entanglement in a Hilbert space with dimension greater than two, is by taking advantage of the diversity of spatial modes of the electromagnetic (EM) field. Furthermore, from modes with well defined OAM, it is possible to generate two-photon states entangled in this degree of freedom, which have a discrete dimensionality as a result of the quantization of angular momentum. The first experimental demonstration of OAM entanglement in photon pairs generated by SPDC was reported in 2001 [8] and since then several similar sources have been implemented.

The role of the linear and nonlinear electromagnetic response of the material used for SPDC on the pump beam is essential for a precise description of the expected quantum correlations of the photon pairs. There is not a unique basis set to perform such a description. Most studies of SPDC rely on the use of the plane EM wave expansion. Accordingly, polarization, linear momentum and frequency become the natural degrees of freedom, and the effects of birefringence on these variables through the type I and type II phase matching conditions restricts the possibility of SPDC by conventional nonlinear crystals. For pump beams with OAM, one may describe the system as a continuum superposition of plane EM waves, or perform the description in terms of modes with OAM. In the latter case it must be recognized that the birefringence of SPDC crystals is able to modify both the polarization and the OAM of the modes that propagate in them[9]. As a consequence, OAM conservation in SPDC does not necessarily hold[10]. Most studies of this kind of effects take as starting point an effective scalar treatment of the EM field and the paraxial description of the pump mode, though going beyond these approximations may lead to observable effects[10–12].

As already reported in Ref. [13], for wide crystals, the plane-wave spectrum from the pump beam results in a multiplicative factor for the transition amplitude of the generated two-photon state. This opens the possibility of using SPDC to generate photons with general properties inherited from the pump photons. In the case of a propagation invariant Bessel pump beam, this could lead to the generation of propagation invariant photons with OAM. In the present work, we theoretically study the circumstances under which this process is feasible and compare our analysis with available experimental results[14].

In section II, we describe general features of type I SPDC involving structured vectorial beams in a birefringent medium. In section III this formalism is applied to the case of a Bessel-Gauss pump beam. Explicit analytical expressions and numerical results for the angular spectrum are given and compared with experimental results. The angular momentum properties of the photon pair are also analyzed, including a discussion on the pertinence of studying its conservation in the SPDC process. Finally, we outline conclusions derived from this study.

II. SPDC OF STRUCTURED EM FIELDS.

Spontaneous parametric down conversion focus on the evolution of an initial state of the quantum electromagnetic field that corresponds to a coherent state for a given pumping mode κ_p with no other occupied mode $|0; \alpha_{\kappa_p}\rangle$, under

the $\hat{\mathcal{H}}_{SPDC}$ Hamiltonian [15],

$$\hat{\mathcal{H}}_{SPDC}|0; \alpha_{\kappa_p}\rangle = \frac{1}{2} \sum_{r,l,t} \int d^3r \chi_{r,l,t}^{(2)} \hat{\mathbf{E}}_r^{(+)} \hat{\mathbf{E}}_l^{(+)} \hat{\mathbf{E}}_t^{(-)} |0; \alpha_{\kappa_p}\rangle \quad (1)$$

$$= \sum_{\kappa^s, \kappa^i} \left[\frac{1}{2} \sum_{r,l,t} \int d^6k_{\perp} \chi_{r,l,t}^{(2)} \mathfrak{E}_{\kappa^s, r}^{(+)}(s^s, k_x^s, k_y^s; \omega^s) \mathfrak{E}_{\kappa^i, l}^{(+)}(s^i, k_x^i, k_y^i; \omega^i) \mathfrak{E}_{\kappa^p, t}^{(-)}(s^p, k_x^p, k_y^p; \omega^p) \right. \\ \left. \times \int d^3r e^{i(\Delta \mathbf{k} \cdot \mathbf{r} - \Delta \omega t)} \hat{a}^\dagger(s^s, k_x^s, k_y^s, \omega^s) \hat{a}^\dagger(s^i, k_x^i, k_y^i, \omega^i) \alpha_{\kappa^p} |0; \alpha_{\kappa^p}\rangle \right]. \quad (2)$$

In this equation the electric fields have been expressed in terms of their transverse spatial Fourier components, so that d^6k_{\perp} encloses the tranverse momentum differentials for each field; $\Delta \mathbf{k}$ denotes the vectorial mismatch term $\Delta \mathbf{k} = \mathbf{k}^p - \mathbf{k}^s - \mathbf{k}^i$, and $\Delta \omega = \omega^p - \omega^s - \omega^i$. Each $\{\kappa^s, \kappa^i\}$ term in this expansion determines the probability amplitude for the creation of a photon in the signal (idler) mode κ^s (κ^i) together with the annihilation of a photon in the coherent pumping state. The time integral of this equation gives an approximate expression, valid within first order perturbation theory, of the time evolved SPDC state

$$|\Psi(t)\rangle = |0; \alpha_{\kappa_p}\rangle + \sum_{\kappa^s, \kappa^i} \left[\frac{1}{2} \sum_{r,l,t} \int d^6k_{\perp} \chi_{r,l,t}^{(2)} \mathfrak{E}_{\kappa^s, r}^{(+)}(s^s, k_x^s, k_y^s; \omega^s) \mathfrak{E}_{\kappa^i, l}^{(+)}(s^i, k_x^i, k_y^i; \omega^i) \mathfrak{E}_{\kappa^p, t}^{(-)}(s^p, k_x^p, k_y^p; \omega^p) \right. \\ \left. \times \int d^3r e^{i(\Delta \mathbf{k} \cdot \mathbf{r} - \Delta \omega t/2)} \text{sinc}(\Delta \omega t/2) \hat{a}^\dagger(s^s, k_x^s, k_y^s, \omega^s) \hat{a}^\dagger(s^i, k_x^i, k_y^i, \omega^i) \alpha_{\kappa^p} |0; \alpha_{\kappa^p}\rangle \right]. \quad (3)$$

In this work we shall present an analysis for a type-I SPDC, with this configuration, for a quasi monochromatic pump beam that propagates in an uniaxial crystal with symmetry axis \mathbf{a} and permeability coefficients ϵ_{\parallel} and ϵ_{\perp} parallel and transversal to the optical axis respectively. The electric field associated to the extraordinary waves is:

$$\mathfrak{E}_{e, \kappa}(\mathbf{k}_x, \mathbf{k}_y; \omega) = \left[-\frac{c^2}{\epsilon_{\perp} \omega^2} \mathbf{k}^e (\mathbf{a} \cdot \mathbf{k}^e) + \mathbf{a} \right] \mathcal{N}_e \alpha(\omega) \tilde{\psi}_{\kappa}(\mathbf{k}_x, \mathbf{k}_y), \quad (4)$$

with $\tilde{\psi}_{\kappa}(\mathbf{k}_x, \mathbf{k}_y)$ the 2-dimensional Fourier transform of the pump beam evaluated at the crystal surface and $\alpha(\omega)$ its spectral envelop. As for the generated photons,

$$\mathfrak{E}_{o, \mathbf{k}_x^0, \mathbf{k}_y^0}(\mathbf{k}_x, \mathbf{k}_y; \omega) = \mathbf{a} \times \mathbf{k}^o \mathcal{N}_o \delta(\mathbf{k}_x - \mathbf{k}_x^0) \delta(\mathbf{k}_y - \mathbf{k}_y^0), \quad (5)$$

if they are described by ordinary vectorial plane waves with wave vector \mathbf{k}^o . In Eqs. (4-5) c denotes the velocity of light in vacuum, \mathcal{N}_e and \mathcal{N}_o are the normalization factors, and the vectors \mathbf{k}^e and \mathbf{k}^o satisfy the extraordinary and the ordinary dispersion relations, respectively.

For a wide crystal the state of the electromagnetic field at asymptotic times can be written as

$$|\Psi\rangle = |0; \alpha_{\kappa_p}\rangle + \int d\omega^s \int d\omega^i \int d^2k_{\perp}^s d^2k_{\perp}^i \mathcal{N}_p \mathcal{N}_s \mathcal{N}_i \alpha(\omega^s + \omega^i) \mathcal{X} F(\mathbf{k}_x^s, \mathbf{k}_y^s; \omega^s, \mathbf{k}_x^i, \mathbf{k}_y^i; \omega^i) |0; \alpha_{\kappa_p}; 1_s; 1_i\rangle. \quad (6)$$

The factor \mathcal{X} results from the contraction of the nonlinear susceptibility tensor $\chi_{r,l,t}^{(2)}$ with the polarization vectors, while the wave vector joint amplitude is defined as

$$F(\mathbf{k}_x^s, \mathbf{k}_y^s; \omega^s, \mathbf{k}_x^i, \mathbf{k}_y^i; \omega^i) = \tilde{\psi}_{\kappa}(\mathbf{k}_x^i + \mathbf{k}_x^s, \mathbf{k}_y^i + \mathbf{k}_y^s) \text{sinc}(L \Delta k_z / 2) \exp(i \Delta k_z L_z / 2). \quad (7)$$

In this equation L denotes the crystal length and $\Delta k_z = k_z^p - k_z^s - k_z^i$, with each k_z evaluated in terms of the vectors \mathbf{k}_{\perp} using the adequate dispersion relation.

The product

$$\mathfrak{F}(\mathbf{k}_x^s, \mathbf{k}_y^s; \omega^s, \mathbf{k}_x^i, \mathbf{k}_y^i; \omega^i) = \alpha(\omega^s + \omega^i) g F(\mathbf{k}_x^s, \mathbf{k}_y^s; \omega^s, \mathbf{k}_x^i, \mathbf{k}_y^i; \omega^i), \quad g = \mathcal{N}_p \mathcal{N}_s \mathcal{N}_i \mathcal{X}, \quad (8)$$

yields the probability amplitude to generate the idler and signal photons and it determines $|\Psi\rangle$ to first order in the perturbation theory. In general, $\mathfrak{F}(\mathbf{k}_x^s, \mathbf{k}_y^s; \omega^s, \mathbf{k}_x^i, \mathbf{k}_y^i; \omega^i)$ will be non negligible for continuous sets of the wave vectors \mathbf{k}_{\perp} , so that the wave function cannot be factorized, and entanglement in continuous and discrete polarization variables can be expected.

Equation (7) shows how the transverse momentum conservation condition $\mathbf{k}_{\perp}^p = \mathbf{k}_{\perp}^i + \mathbf{k}_{\perp}^s$ induces the transfer of the plane-wave spectrum from the pump beam to the two-photon state[13]. If, for instance, one of the photons in the pair

is projected in a state with a well defined value of \mathbf{k}_\perp , the other photon will have an angular spectrum proportional to the pump spectrum with an argument modified by a constant additive term. Note, however, that \mathfrak{F} is also modulated both by the longitudinal phase matching factor (which depends on \mathbf{k}_\perp^i and \mathbf{k}_\perp^s by the dispersion relations) and by the nonlinear response term \mathcal{X} . Thus, the conditions under which the idler and/or signal photons inherit general features of the pump beam angular spectra are not evident.

An important function to calculate is the angular spectrum (AS), which describes the distribution of signal photons in the wave vector domain, and is defined as

$$R_s(\mathbf{k}_0^s) = \int d\omega^i \int d^2k_\perp^i |\mathfrak{F}(\mathbf{k}_{x,0}^s, \mathbf{k}_{y,0}^s; \omega^s, \mathbf{k}_x^i, \mathbf{k}_y^i; \omega^i)|^2. \quad (9)$$

The conditional angular spectrum (CAS), which is a function of \mathbf{k}_\perp^s and \mathbf{k}_\perp^{i0} , is defined as:

$$R_c(\mathbf{k}_\perp^s, \mathbf{k}_\perp^{i0}) = \int d\omega^i |\mathfrak{F}(\mathbf{k}_x^s, \mathbf{k}_y^s; \omega^s, \mathbf{k}_{x,0}^i, \mathbf{k}_{y,0}^i; \omega^i)|^2, \quad (10)$$

and represents the probability to detect an idler photon with wave vector \mathbf{k}_\perp^{i0} in coincidence with a signal photon with wave vector \mathbf{k}_\perp^s . Under a realistic situation involving small but finite transverse dimensions of the pump beam and a usually wide but not so long crystal, there is a set of relevant pump wave vectors \mathbf{k}^p that are close to satisfy the phase matching condition $\Delta k_z = 0$ for a given idler wave vector \mathbf{k}^i .

III. SPDC FOR A PROPAGATION INVARIANT PUMP WITH CIRCULAR CYLINDER SYMMETRY.

The solutions of the scalar wave equation that preserve its amplitude along a main propagation axis and have well defined orbital angular momentum are known as Bessel modes. Under ideal conditions for a pump Bessel field of ℓ -th order and transverse wave number κ_\perp^p , propagating along the z -axis, the corresponding scalar spectra is given by

$$\tilde{\psi}_\kappa(\mathbf{k}_x, \mathbf{k}_y) = i^\ell e^{i\ell\varphi_{\kappa_\perp}} \delta(\mathbf{k}_\perp^p - \kappa_\perp^p) / \kappa_\perp^p. \quad (11)$$

Approximate realizations of Bessel beams in the laboratory correspond to superpositions of waves with vectors \mathbf{k} in a narrow conic shape volume:

$$\delta(\mathbf{k}_\perp^p - \kappa_\perp^p) \rightarrow \frac{1}{W\sqrt{2\pi}} \text{Exp} [-(\mathbf{k}_\perp^p - \kappa_\perp^p)^2 / 2W^2], \quad W \ll \kappa_\perp^p. \quad (12)$$

with W the beam waist parameter. In the literature these modes are called Bessel-Gauss modes.

Consider a linearly polarized Bessel-Gauss mode generated in free space. The beam is sent with its main direction of propagation along the z -axis, *i. e.*, perpendicular to the crystal surface and with a polarization vector within the extraordinary plane (the axis of birefringence will be taken as $\mathbf{a} = (0, a_y, a_z)$). The angular spectra of the scalar pump beam \mathfrak{E}^{sc} can be approximately expressed as[16]:

$$\mathfrak{E}_{\mathbf{k}_\perp^p, \ell, \omega}^{sc} \sim \mathcal{E}^{sc} \frac{e^{-(\mathbf{k}_\perp^p - \kappa_\perp^p)^2 / 2W^2}}{\kappa_\perp^p} e^{i\ell\varphi_{\kappa_\perp^p}} \hat{\mathbf{e}}_y. \quad (13)$$

Inside the crystal the extraordinary mode that will give rise to the SPDC process would evolve according to Eq. (4) with an amplitude determined approximately by $\mathfrak{E}^{sc} \cdot \mathfrak{E}_\kappa$. For uniaxial media, the nonlinear optical susceptibilities $\chi_{r,l,t}^{(2)}$ are usually reported in the reference frame where the birefringent axis is taken as the z -axis. In this frame we can evaluate \mathcal{X} , and then translate the results in terms of the rotated wave vector \mathbf{k} . Let us take as a particular example the case of a beta barium borate (BBO) crystal and a type I phase-matching configuration. The symmetry of the crystal is such that, in the crystal natural frame ($\hat{\mathbf{e}}_3 = \mathbf{a}$):

$$\mathcal{X} \approx -d_{22} \left[[\hat{\mathbf{e}}_x^0 \hat{\mathbf{e}}_y^0 + \hat{\mathbf{e}}_y^0 \hat{\mathbf{e}}_x^0] \hat{\mathbf{e}}_x^e + [\hat{\mathbf{e}}_x^0 \hat{\mathbf{e}}_x^0 - \hat{\mathbf{e}}_y^0 \hat{\mathbf{e}}_y^0] \hat{\mathbf{e}}_y^e \right]. \quad (14)$$

In the case of vectorial electromagnetic beams in birefringent crystals, the components of the electric field depend on the components of the wave vector, Eqs. (4-5), so that,

$$\mathcal{X} \approx -d_{22} \frac{\omega^s}{c} \frac{\omega^i}{c} \tilde{k}_z^p \left[[-\tilde{k}_y^s \tilde{k}_x^i - \tilde{k}_x^s \tilde{k}_y^i] \tilde{k}_x^p + [\tilde{k}_y^s \tilde{k}_y^i - \tilde{k}_x^s \tilde{k}_x^i] \tilde{k}_y^p \right], \quad (15)$$

with $\tilde{\mathbf{k}}$ the rotated wave vector in the crystal reference frame.

For the system under consideration, if the crystal is wide and the pump beam satisfies the paraxial condition, $k_\perp^p \ll \omega/c$, the conservation of transversal momentum makes reasonable that both the relevant ordinary and extraordinary modes are quasi parallel to the incident beam. All these considerations make feasible to replace the vectorial factor \mathcal{A} by its effective value \mathcal{A}_{eff} . This implies that under these conditions, the SPDC process of structured paraxial beams will be determined just by the scalar potential $\tilde{\psi}^p$ modulated by the longitudinal phase matching factor. Notice, however, these considerations also suggest that the usage of vectorial non paraxial beams could open new perspectives in SPDC.

A. Angular spectrum and conditional angular spectrum for paraxial scalar Bessel beams.

In this subsection we calculate the AS and CAS functions for a quasi paraxial scalar Bessel pump beam, Eq. (13), under the conditions described in the last paragraph.

The first observation is that the modulus of the joint amplitude $|\mathfrak{F}|$, Eq. (8), in the scheme where Eq. (13) is valid, does not depend on ℓ . So that the AS and CAS are ℓ independent[17].

We assume type-I SPDC in an uniaxial birefringent crystal with its optical axis given by $\mathbf{a} = (0, a_y, a_z)$. For degenerated emission, i.e., $\omega^p = \omega = 2\omega^s = 2\omega^i$, the emitted photons dispersion relation is

$$k_{z,b}^O = \sqrt{\epsilon_\perp \omega^2 / 4c^2 - (k_\perp^b)^2} \quad b = i, s, \quad (16)$$

with the ordinary refraction index $n_o = \sqrt{\epsilon_\perp}$. The dispersion relation for the pump wave which evolves in the extraordinary plane is

$$k_z^E(\mathbf{k}_\perp, \omega) = -\beta \mathbf{a} \cdot \mathbf{k}_\perp + \frac{\omega}{c} n_{eff} \sqrt{1 - \frac{k_\perp^2 c^2}{\omega^2}} \eta, \quad (17)$$

$$n_{eff} = \sqrt{\frac{\epsilon_\perp \epsilon_\parallel}{\epsilon_\perp + \Delta \epsilon a_z^2}}, \quad \beta = \frac{\Delta \epsilon a_z}{\epsilon_\perp + \Delta \epsilon a_z^2}, \quad (18)$$

$$\eta = \frac{1}{\epsilon_\parallel} + \frac{\Delta \epsilon}{\epsilon_\perp \epsilon_\parallel} (1 - a_z \beta) (\mathbf{a} \cdot \hat{\mathbf{k}}_\perp)^2, \quad (19)$$

where $\Delta \epsilon = \epsilon_\parallel - \epsilon_\perp$.

In order to obtain approximate expressions for the AS function, we make a first order Taylor description of the phase mismatch term,

$$\Delta k_z \sim \tilde{\kappa} - \mathbf{d} \cdot (\mathbf{k}_\perp^s + \mathbf{k}_\perp^i), \quad (20)$$

with

$$\tilde{\kappa} = (\omega/c)(n_{eff} - n_o) + (2c/n_o\omega)(k_\perp^s)^2, \quad (21)$$

$$\mathbf{d} = \beta \mathbf{a}_\perp + (2c/n_o\omega) \mathbf{k}_\perp^s. \quad (22)$$

Writing the pump integration variable \mathbf{k}_\perp^p in polar coordinates, and performing a rotation of the integration variable by an angle $\theta_r = \arccos(d_x/|\mathbf{d}|)$, the expression for the AS can be written in terms of a single integral:

$$R_s(k_x^s, k_y^s) \sim |g\alpha(\omega_p)|^2 e^{-\sigma_{AS}^{-2}((k_\perp^s)^2 - r_{AS}^2)^2} \int_0^{2\pi} \text{Exp} \left[-\frac{(\gamma L)^2}{2} (|\mathbf{d}| \kappa_\perp^p \cos \theta - \tilde{\kappa})^2 \right] d\theta, \quad (23)$$

$$r_{AS}^2 = \frac{1}{2} \left(\frac{n_o \omega}{c} \right)^2 \left(1 - \frac{n_{eff}}{n_o} \right), \quad \sigma_{AS}^{-2} = 2(\gamma L c / n_o \omega)^2$$

To obtain this expression, we have approximated the function $\text{sinc}(x)$ by a Gaussian function $\exp[-(\gamma x)^2]$, $\gamma = 0.4393$. We have also taken the limit $W \rightarrow 0$ with the restriction of a finite pump intensity. According to Eq. (23), for $\kappa_\perp^p \ll (\omega/c)(n_{eff} - n_o)$, the AS is concentrated in a cone given by the condition $k_\perp^s = (n_o \omega / \sqrt{2} c) \sqrt{1 - n_{eff}/n_o}$ (a similar expression is obtained for Gaussian pump beams [18]). The cone width is approximately given by $\sqrt{n_o \omega / \sqrt{2} \gamma L c}$. Notice that the dependence of $|\mathbf{d}|$ on the orientation of the axis \mathbf{a} , Eq. (22), is a source of an anisotropy for the AS ring that becomes more relevant as κ_\perp^p increases.

Our theoretical scheme has been implemented using parameters from the reported experimental setup in Ref. [14]. We consider a SPDC source based on a BBO crystal, cut for type-I phase matching for degenerated emission at a pump wavelength centered at 406.8 nm ($\theta_a = 29.3^\circ$). The numerical simulations consider monochromatic Bessel-Gauss pump beams with a waist $W = 0.0007\mu\text{m}^{-1}$ and three different values for the transverse wave number parameter $\kappa_\perp^p = 0.05, 0.09, 0.15\mu\text{m}^{-1}$. They are performed both using the complete expression of the transition rate Eq.(9) without resorting approximations to the dispersion relations, Figs. 1a-1c, and using the analytic expression, Eq. (23), Figs. 1b-1d, for two different crystal lengths. The AS function for $\kappa_\perp^p = 0.05\mu\text{m}^{-1}$ shows an asymmetry compatible with the experimental results reported in Ref.[14]. In this case, the AS function is concentrated in a cone of radius $0.49\mu\text{m}^{-1}$ and width between $\sim 0.01 - 0.03\mu\text{m}^{-1}$ dependent on k_y^s/k_x^s . Both radius and width are within the expectations described in the last paragraph. As κ_\perp^p increases, the anisotropies are more visible and the spectra is better described by two non concentric cones. This is illustrated in Fig.(1a)B where $\kappa_\perp^p = 0.09\mu\text{m}^{-1}$ and Fig.(1a)C with $\kappa_\perp^p = 0.15\mu\text{m}^{-1}$. As the crystal length is increased the regions where the AS has significant values are smaller and the anisotropy associated to the extraordinary pump beam dispersion relation is more evident. This, along with the oscillatory behavior of the sinc function, leads to a higher structured landscape for the AS function; which, nevertheless is still concentrated in two narrow non concentric cones. The radius of the external cone increases as κ_\perp increases while the radius of the internal cone decreases as κ_\perp decreases. By comparing Figs. 1a with Figs. 1b and Figs. 1c with Figs. 1d we can conclude that the analytic expression, Eq.(23), reproduces the general features of the AS function for κ_\perp^p at least as high as $0.15\mu\text{m}^{-1}$.

Using the same approximations for the phase matching function and phase mismatch term, it is possible to obtain a useful expression for the CAS function. In this case we do not take the limit $W \rightarrow 0$ to make more explicit the role of this parameter in the expected CAS to be measured in the laboratory. Replacing Eq.(7), Eq.(13) and Eq.(20) in Eq.(10), for degenerate SPDC, we obtain:

$$R_c(\mathbf{k}_\perp^s, \omega^s; \mathbf{k}_\perp^i, \omega^i) \sim \frac{|g\alpha(\omega^p)|^2}{2\pi W^2} e^{-((\mathbf{k}_\perp^s - \mathbf{K}_\perp^0)^2 - \mathcal{R}_\mathbf{k}^2)/2W_{eff}^2}, \quad (24)$$

with

$$\begin{aligned} W_{eff}^{-2} &= W^{-2} + \gamma^2 L^2 \beta^2 (\hat{\mathbf{a}} \cdot \hat{\mathbf{k}}_\perp)^2, \\ \mathbf{K}_\perp^0 &= -\frac{W_{eff}^2}{W_\mathbf{k}^2} \mathbf{k}_\perp^i + (\gamma L W_{eff})^2 \left(\frac{\omega}{c} (n_{eff} - n_o) - \beta \mathbf{a} \cdot \mathbf{k}_\perp^i \right) \left(\frac{2c}{n_o \omega} \mathbf{k}_\perp^i - \beta \mathbf{a} \right), \\ \mathcal{R}_\mathbf{k}^2 &= \frac{W_{eff}^2}{W^2} (\kappa_\perp^p)^2 + (\mathbf{k}_\perp^i)^2 \left[\frac{W_{eff}^4}{W^4} - \frac{W_{eff}^2}{W^2} \right] + 2(\gamma L W_{eff})^2 \left(\frac{\omega}{c} (n_{eff} - n_o) - \beta \mathbf{a} \cdot \mathbf{k}_\perp^i \right) \left(\frac{2c}{n_o \omega} (\mathbf{k}_\perp^i)^2 - \beta \mathbf{a} \cdot \mathbf{k}_\perp^i \right) \\ &\quad - \left(\frac{2c}{n_o \omega} (\mathbf{k}_\perp^i)^2 - \beta \mathbf{a} \cdot \mathbf{k}_\perp^i \right)^2 (\gamma L W_{eff})^2 \left[1 - (\gamma L W_{eff})^2 \left| \frac{2c}{n_o \omega} \mathbf{k}_\perp^i - \beta \mathbf{a} \right|^2 \right]. \end{aligned} \quad (25)$$

If the crystal is not too long $W_{eff} \sim W$, $\mathbf{K}_\perp^0 = -\mathbf{k}_{\perp,i}$ and $\mathcal{R}_\mathbf{k} \sim k_\perp^0$, as the length of the crystal increases the longitudinal phase matching condition becomes more relevant and two types of corrections arises. One of them is related to the differences between the extraordinary and ordinary refractive indices and the other includes effects of the orientation of the birefringent axis \mathbf{a} and is thus highly anisotropic. The latter can be related to the spatial walk-off. Both effects make that the signal photon contributes to observable differences between the general characteristics of the signal photon with respect to the pump photon. Notice, however, that the structure of Eq. (24) is that of an approximate propagation invariant signal photon, as reported in reference [14], whenever $\mathcal{R}_\mathbf{k}^2 > 0$.

In the idealized limit of $W \rightarrow 0$, *i. e.*,

$$\begin{aligned} R_c(\mathbf{k}_\perp^s, \omega^s; \mathbf{k}_\perp^i, \omega^i) &\rightarrow \frac{|g\alpha(\omega_p)|^2}{k_\perp^0} \delta(|\mathbf{k}_\perp^s + \mathbf{k}_\perp^i| - \kappa_\perp^p) \times \\ &\quad \text{Exp} \left[-\gamma^2 L^2 \left(2(\mathbf{k}_\perp^i + \mathbf{k}_\perp^s) \cdot \left(\frac{2c}{n_o \omega} \mathbf{k}_\perp^i - \beta \mathbf{a} \right) \left(\frac{\omega}{c} (n_{eff} - n_o) - \beta \mathbf{a} \cdot \mathbf{k}_\perp^i \right) + \frac{\omega}{c} (n_{eff} - n_o) - \beta \mathbf{a} \cdot \mathbf{k}_\perp^i \right)^2 \right], \end{aligned} \quad (26)$$

The condition of propagation invariance for a beam with main propagation axis along $(2c/\omega n_o)(-\mathbf{k}_\perp^i, k_z^i)$ can be written as

$$\left[\frac{k_z^i}{k_\perp^i k_0^i} (\mathbf{k}_\perp^i \cdot \mathbf{k}_\perp^s) + \frac{k_\perp^i k_z^s}{k_0^i} \right]^2 + \left[\frac{\mathbf{k}_\perp^i \times \mathbf{k}_\perp^s}{k_\perp^i} \right]^2 = (\kappa_\perp^p)^2, \quad k_0^i = n_o \omega^i / c = |\mathbf{k}^i|; \quad (27)$$

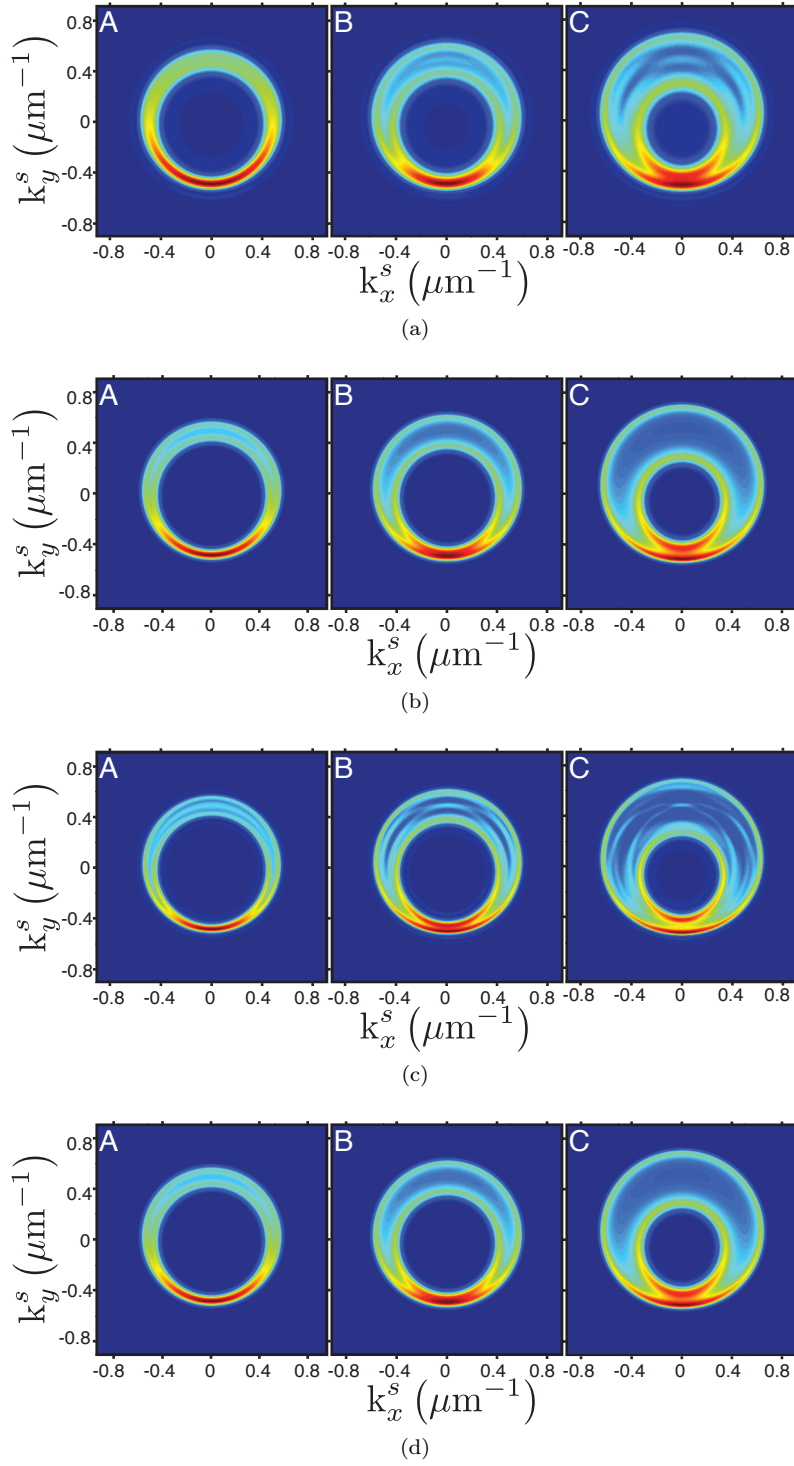


Figure 1: Angular spectrum (AS) for a pump beam with a waist $W = 0.0007\mu\text{m}^{-1}$ and different values of transverse wave number: (A) $\kappa_{\perp}^p = 0.05\mu\text{m}^{-1}$; (B) $\kappa_{\perp}^p = 0.09\mu\text{m}^{-1}$; (C) $\kappa_{\perp}^p = 0.15\mu\text{m}^{-1}$. Figures (a) and (b) consider a 1 mm long BBO crystal while in (c) and (d) the crystal length is increased to 2mm. In figures (a) and (c), the AS is calculated numerically through Eq.(8), while in figures (b) and (d) the AS is calculated from the analytic expression Eq.(23). The optical axis of the crystal is located in the Y-Z plane.

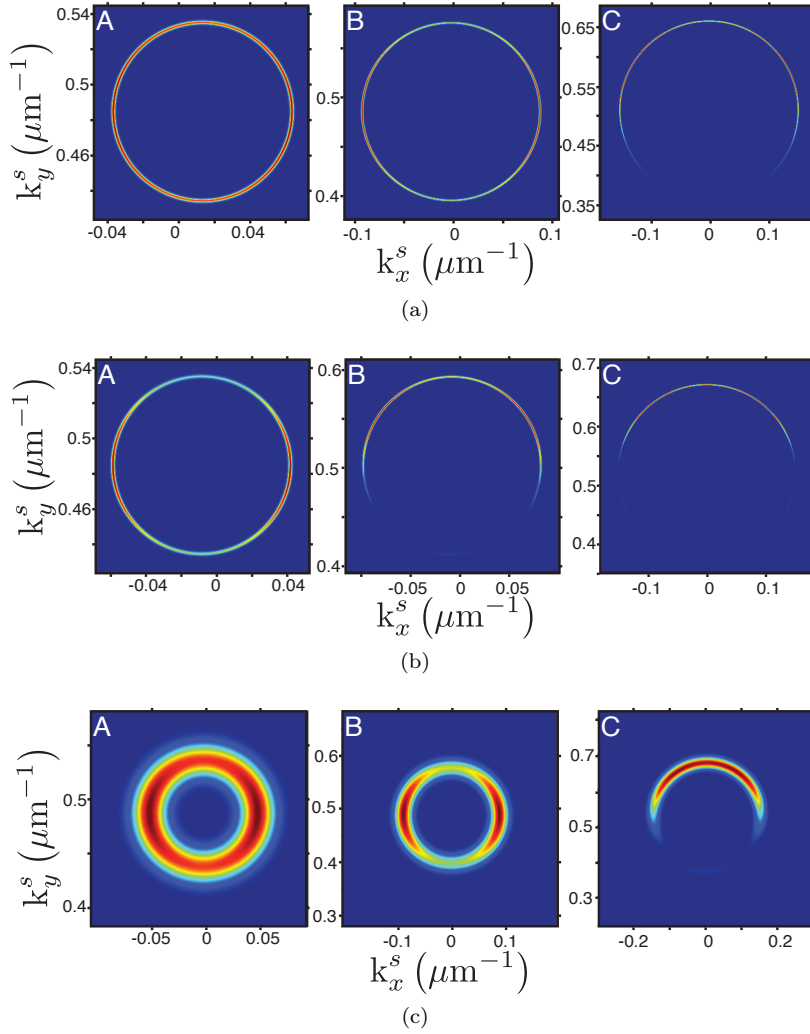


Figure 2: Maximal conditional angular spectrum for a pump Bessel Gauss beam with waist $W = 0.0007\mu\text{m}^{-1}$ in Figs. (a) and (b) and $W = 0.007\mu\text{m}^{-1}$ in Fig. (c). The transverse wave numbers are: (A) $\kappa_{\perp}^p = 0.05\mu\text{m}^{-1}$, (B) $\kappa_{\perp}^p = 0.09\mu\text{m}^{-1}$, and (C) $\kappa_{\perp}^p = 0.15\mu\text{m}^{-1}$. The crystal length is 1 mm in Figs. (a) and (c) and 2 mm in Fig. (b).

expression that can be written in the form

$$|\mathbf{k}_{\perp}^s + \mathbf{k}_{\perp}^i|^2 \left(\frac{\omega^i}{\omega^s} \right)^2 + (k_{\perp}^s)^2 \left[1 - \left(\frac{\omega^i}{\omega^s} \right)^2 \right] - \frac{(k_{\perp}^s)^2}{(k_0^i)^2} \left[(\mathbf{k}_{\perp}^i \cdot \hat{\mathbf{k}}_{\perp}^s)^2 + (k_{\perp}^i)^2 + \mathbf{k}_{\perp}^i \cdot \mathbf{k}_{\perp}^s \right] = \kappa_{\perp}^2. \quad (28)$$

As a consequence, the degenerate SPDC leads to approximate propagation invariant photons whenever $k_{\perp}^s \ll |\mathbf{k}^s|$. As we have shown, for paraxial pump beams, the mean radii of the emission cone is determined by the difference between refractive indices, while the radius κ_{\perp} coincides with that of the pump Bessel beam. Under the experimental conditions reported in Ref. [14] $k_{\perp}^s/|\mathbf{k}^s| \sim 0.1$.

We now illustrate the CAS function for the same general parameters used in Fig. 3, taking the transversal wave vector of the idler photon $\mathbf{k}_{\perp}^{i,max}$ that maximizes the counts in the AS, and name it "maximal CAS". In the case reported in Fig.(1a)A, the maximum AS corresponds to $\mathbf{k}_{\perp}^{i,max} = (0.027, -0.485)\mu\text{m}^{-1}$ and Fig.(2a) shows the corresponding maximal CAS. As expected this function is centered at the opposite value of $\mathbf{k}_{\perp}^{i,max}$ and gives rise to a ring with a radius approximately equal to the corresponding κ_{\perp}^p . Increasing the value of κ_{\perp}^p the maximal CAS is still concentrated in a ring with a radius approximately equal to the corresponding κ_{\perp}^p , but the distribution is not uniform. The width of the ring is approximately equal to the width in wave vector space of the incident beam with an slight dependence on the crystal length, see Fig.(2b). Fig. 2c illustrates the maximal CAS for an incident pump beam with a waist $W = 0.007\mu\text{m}^{-1}$; it shows in greater detail its anisotropic transversal structure as a function of κ_{\perp}^p . The similarity

with the experimental results reported in Ref.[14] is also evident. According to the discussion presented before, we conclude that the emitted signal photons will be approximately propagation invariant in all the studied cases; though the intensity structure in coordinate space may be highly anisotropic in the transversal plane.

B. Post selected photons with well defined angular momentum along different propagation axes.

In this subsection we consider the same general set up described in the previous subsection. Now we evaluate the emission probability of photon pairs each of which has a Bessel-Gauss structure. The calculation is made by a direct integration of Eq. (6) with the structured pump beam described by Eq. (4), and the idler and signal photons with the proper structure factor

$$\mathfrak{E}_{O,\kappa}(\mathbf{k}_x, \mathbf{k}_y; \omega) = \mathbf{a} \times \mathbf{k}^O \tilde{\psi}_\kappa(\mathbf{k}_x, \mathbf{k}_y). \quad (29)$$

According to the results of last section, the main propagation axis of the post selected signal and idler Bessel photons is expected to differ from the pump beam axis. For a pump field close to satisfy the paraxial approximation, $\kappa_\perp^p \ll k_z^p$, this joint probability is expected to be maximal for photons with their main propagation axis nearby the cone with squared radius $r_{AS}^2 = (n_o \omega / c)^2 (1 - n_{eff} / n_o) / 2$ in wave vector space.

Given a scalar Bessel beam with main propagation axis

$$\hat{p}_3 = (\sin \tilde{\theta} \cos \tilde{\varphi}, \sin \tilde{\theta} \sin \tilde{\varphi}, \cos \tilde{\theta}), \quad (30)$$

the vectors

$$\hat{p}_1 = (\cos \tilde{\theta} \cos \tilde{\varphi}, \cos \tilde{\theta} \sin \tilde{\varphi}, -\sin \tilde{\theta}), \quad (31)$$

$$\hat{p}_2 = (-\sin \tilde{\varphi}, \cos \tilde{\varphi}, 0), \quad (32)$$

together with (30) form an orthogonal basis on which any vector \mathbf{k} , with components (k_x, k_y, k_z) in the frame where the normal of the surface of the crystal coincides with the z -axis, has components

$$\begin{aligned} \tilde{k}_x &= k_x \cos \tilde{\theta} \cos \tilde{\varphi} + k_y \cos \tilde{\theta} \sin \tilde{\varphi} - k_z \sin \tilde{\theta} \\ \tilde{k}_y &= -k_x \sin \tilde{\varphi} + k_y \cos \tilde{\varphi} \end{aligned} \quad (33)$$

$$\tilde{k}_z = k_x \sin \tilde{\theta} \cos \tilde{\varphi} + k_y \sin \tilde{\theta} \sin \tilde{\varphi} + k_z \cos \tilde{\theta}. \quad (34)$$

In the basis $\{\hat{p}_1, \hat{p}_2, \hat{p}_3\}$ the scalar factor of the Bessel mode is

$$\psi_{\hat{p}_3; \kappa_\perp, \ell}(\tilde{\mathbf{r}}) = \int d^3 \tilde{k} e^{i \tilde{\mathbf{k}} \cdot \tilde{\mathbf{r}}} \delta(\tilde{k}_z - \tilde{K}_z(\omega, \tilde{k}_\perp)) \frac{\delta(\tilde{k}_\perp - \kappa_\perp)}{\kappa_\perp} i^\ell e^{i \ell \tilde{\varphi}} \quad (35)$$

with \tilde{K}_z given by the adequate dispersion relation, Eqs. (16- 17). Writing the vector $\tilde{\mathbf{k}}$ in terms of (k_x, k_y, k_z) , and using that $\tilde{\mathbf{k}} \cdot \tilde{\mathbf{r}} = \mathbf{k} \cdot \mathbf{r}$, we can get an expression for $\tilde{\psi}_{\hat{p}_3; \kappa_\perp, \ell}(\mathbf{k}_x, \mathbf{k}_y)$. For an ordinary Bessel mode it results

$$\begin{aligned} \tilde{\psi}_{\hat{p}_3; \kappa_\perp, \ell}^{(O)}(\mathbf{k}) &= \pm \frac{k_\perp^{|\ell|}}{\kappa_\perp^{|\ell|}} \frac{\delta(k_z - K_z^{(O)}(\omega_B, \kappa_\perp, \tilde{\theta}; \varphi))}{\kappa_\perp} \frac{\delta(k_\perp - K_\perp^{(O)}(\kappa_\perp, \omega_B, \tilde{\theta}; \varphi))}{\text{Jac}^{(O)}(\kappa_\perp, \omega_B, \tilde{\theta}; \varphi)} \\ &\times \sum_{m=0}^{|\ell|} \binom{|\ell|}{|\ell| - m} \left(\cos \tilde{\theta} \cos(\varphi - \tilde{\varphi}) + i \frac{\ell}{|\ell|} \sin(\varphi - \tilde{\varphi}) \right)^m \left(-\frac{k_z}{k_\perp} \sin \tilde{\theta} \right)^{|\ell| - m}. \end{aligned} \quad (36)$$

$$K_z^{(O)}(\kappa_\perp, \omega_B; \varphi; \tilde{\theta}; \tilde{\varphi}) = \left[\frac{\sqrt{\epsilon_\perp \omega_B^2 / c^2 - \kappa_\perp^2}}{\cos \tilde{\theta}} \right]$$

$$\pm |\tan \tilde{\theta} \cos(\tilde{\varphi} - \varphi)| \sqrt{\kappa_\perp^2 / \cos^2 \tilde{\theta} - (\epsilon_\perp \omega_B^2 / c^2) \tan^2 \tilde{\theta} \sin^2(\tilde{\varphi} - \varphi)} / (1 + \tan^2 \tilde{\theta} \cos^2(\tilde{\varphi} - \varphi)), \quad (37)$$

$$K_\perp^{(O)}(\kappa_\perp, \omega_B; \varphi; \tilde{\theta}; \tilde{\varphi}) = \sqrt{\epsilon_\perp \omega_B^2 / c^2 - K_z^{(O)2}}, \quad (38)$$

and the Jacobian term is

$$\text{Jac}^{(O)}(\omega_B; \mathbf{k}_\perp; \varphi; \tilde{\theta}, \tilde{\varphi}) = \frac{|\mathbf{k}_\perp - \mathbf{k}_z \cos(\tilde{\varphi} - \varphi) \sin \tilde{\theta}|}{\kappa_\perp}. \quad (39)$$

The dependence of the relevant values of \mathbf{k}_z and \mathbf{k}_\perp , $K_z^{(O)}$ and $K_\perp^{(O)}$, on the angle φ reflects the elliptic shape of the beam in the wave vector plane defined by a constant value of \mathbf{k}_z . The ordinary dispersion relation term $\sqrt{\epsilon_\perp \omega_B^2/c^2 - \kappa_\perp^2}$ is a direct measure of the electromagnetic momentum of the Bessel beam along the \hat{p}_3 axis. $K_z^{(O)}$ is proportional to the momenta along the z -axis; κ_\perp determines directly the radial momenta of ordinary photons perpendicular to the \hat{p}_3 axis; the Jacobian terms Eq. (39) are a consequence of the conceptual difference between \mathbf{k}_\perp and κ_\perp . Note that the effective dispersion relation for the Bessel mode, Eq. (37) gives real values just for values of the angular variable φ satisfying $|\kappa_\perp| \geq |(n_o \omega_B/c) \sin \tilde{\theta}|$. The summation terms in Eq. (36) substitute the $e^{i\ell\varphi}$ term that would arise for a Bessel beam propagating along the \hat{e}_3 -axis. Notice that similar terms arise in the description of SPDC for other beams exhibiting orbital angular momentum as, for instance, Laguerre Gaussian beams [10].

The transition amplitude of the generation of a signal Bessel photon with angular momenta ℓ^s and transverse wave number κ_\perp^s along with an idler Bessel photon with angular momenta ℓ^i and transverse wave number κ_\perp^i is proportional to

$$F(\ell^p, \kappa_\perp^p, \omega^p; \ell^s, \kappa_\perp^s, \omega^s; \ell^i, \kappa_\perp^i, \omega^i) = \int d^3\mathbf{k}^s \int d^3\mathbf{k}_i \tilde{\psi}_{\hat{e}_3; \kappa_\perp^p, \ell^p}^{(E)}(\mathbf{k}_\perp^i + \mathbf{k}_\perp^s; \ell^p) \tilde{\psi}_{\hat{p}^s; \kappa_\perp^s, \ell^s}^{(O)}(\mathbf{k}_\perp^s) \tilde{\psi}_{\hat{p}^i; \kappa_\perp^i, \ell^i}^{(O)}(\mathbf{k}_\perp^i) \text{sinc}(L\Delta\mathbf{k}_z/2); \quad (40)$$

the proportionality factor $g = |\alpha| \mathcal{N}_p \mathcal{N}_s \mathcal{N}_i \mathcal{X}_{eff}$ involves the pump coherent amplitude α , the normalization factors of the pump, idler and signal photons as well as the effective nonlinear susceptibility adequate to the scalar pump beam.

According to the results of last section, the transition amplitude will become maximal if the signal photon has an orientation axis $\hat{p}_3^{(s)}$ determined by the maxima in the AS function, while the orientation of the idler photon corresponds to $\tilde{\theta}_i = \theta_s$ and $\tilde{\varphi}_i = \tilde{\varphi}_s + \pi$ provided that $\kappa_\perp^s \ll \kappa_\perp^i$. Notice that this implies that the idler and signal photons can already be distinguished by their perpendicular wave vector.

In Figs. 3 and 4 we illustrate the behavior of the conditional amplitudes as a function of the angular momentum of the pump photon as well as a function of its transverse wave vector. In those figures we also illustrate the dependence on the orientation of the resulting idler and signal photons. To make the results closer to expected experimental realizations, the calculations were performed with Bessel-Gauss modes with an small waist $W = 0.0005 \mu\text{m}^{-1}$. The crystal properties are the same as in the illustrative examples of the CAS and AS distributions in last section. As could be inferred from the results obtained for the CAS, smaller values of the pump transverse vector κ_\perp^p yield a more localized distribution of the OAM of the photon pair. That is, pump beams that can be closely described by the paraxial approximation can be used to generate photon pairs with few relevant values of ℓ^i and ℓ^s . In particular, a paraxial pump beam with $\ell^p = 0$ will yield mainly photon pairs without OAM along their propagation axis. For pump beams with bigger κ_\perp^p it is predicted a high correlation between the angular momentum of the idler and signal photons involving a broad but well defined values ℓ^i and ℓ^s along a straight line. This property is perserved whether the structured photon pairs are detected in the direction of maximal CAS (first row in Figs. 3 and 4) or in any other orientation as illustrated in the second row in Figs. 3 and 4. For paraxial beams, the maximum transition rates for an orientation perpendicular to that of maximal CAS is approximately half of the maximum values found along the maximal CAS. Notice that as the orbital angular momentum is evaluated along diferent axes for the idler, signal and pump photons, it does not make strict sense to talk about conservation of OAM by comparing $\ell^i + \ell^s$ with ℓ^p . Nevertheless we can observe that the greatest transition rates in the non paraxial regime, Fig. 4, are along straight lines that go through the origin for $\ell^p = 0$, pass through $|\ell^i| = 1$ and $\ell^s = 0$ for $\ell^p = 1$, and pass through $|\ell^i| = 2$ and $\ell^s = 0$ for $\ell^p = 2$.

Finally, in Fig. 5, the marginal distributions of the idler and signal orbital angular momentum are illustrated. They were evaluated for a paraxial pump beam with the same set up as in Fig. 3. For the photon in the pair with the same value of κ_\perp than the pump beam, i. e., for idler photon, the OAM marginal distribution has clearly an oscillatory behavior dependent on the parity of the ℓ^i for $-15 \leq \ell^i \leq 15$. Meanwhile, for the photon with lower value of κ_\perp this behavior is observed for a much smaller ℓ^s interval.

IV. CONCLUSIONS

In this paper, it has been shown that SPDC can be used to generate structured photons with several predetermined properties inherited from the pump beam. We have found that the use of scalar pump fields that are approximately

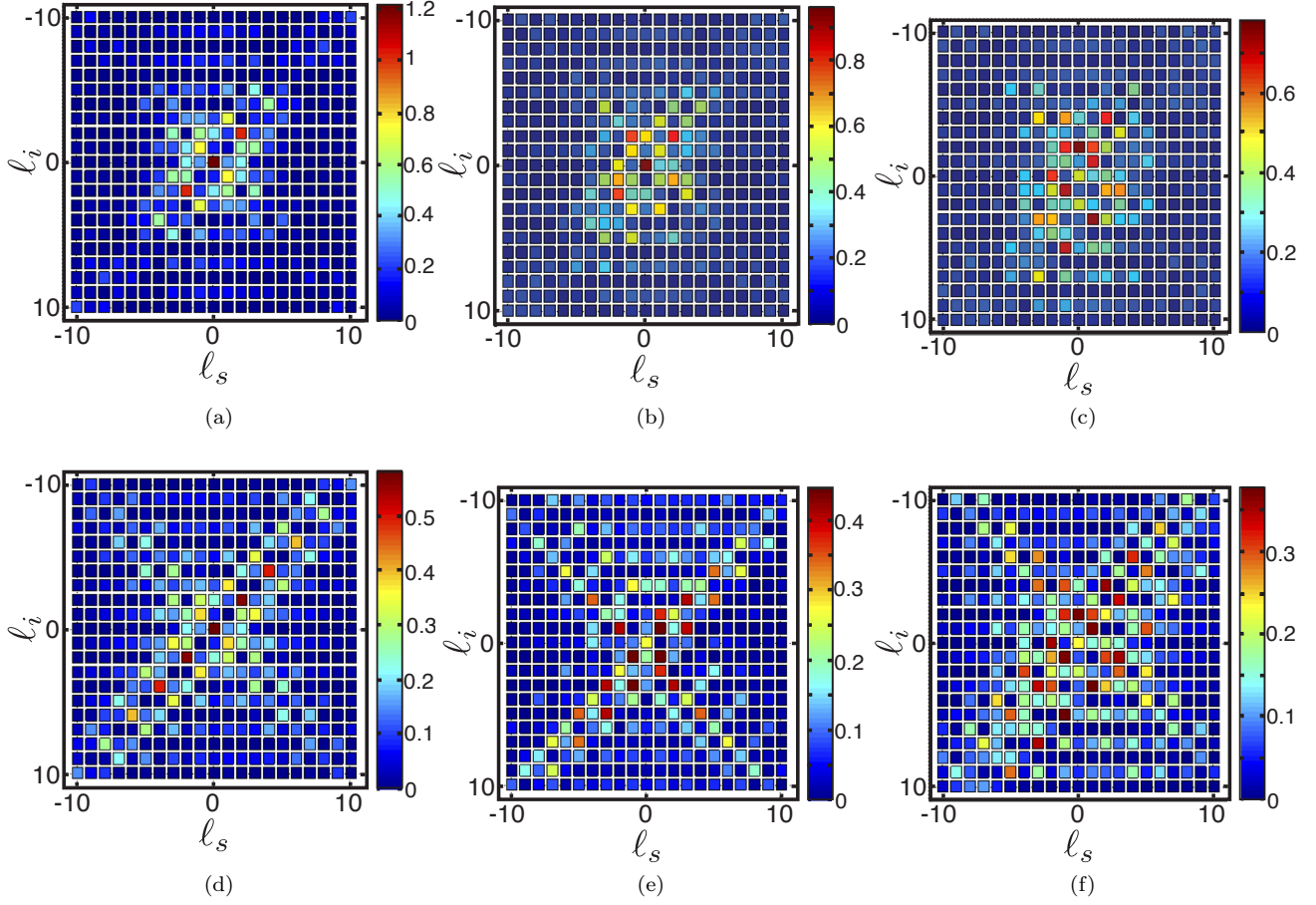


Figure 3: Modulus of the transition element F , Eq. (40), as a function of the orbital angular momentum of the signal ℓ^s and idler ℓ^i photon. They involve a pump Bessel Gauss photon with transverse wave number $\kappa_{\perp}^p = 0.01\mu\text{m}^{-1}$, a signal Bessel photon with $\kappa_{\perp}^s = 0.0001\mu\text{m}^{-1}$ and an idler photon with $\kappa_{\perp}^i = 0.01\mu\text{m}^{-1}$. The idler and signal photons are emitted with their main propagation axis with orientation angles $\tilde{\theta} = \theta_{ec}$ and $\tilde{\varphi}_s = -\pi/2$ and $\tilde{\varphi}_i = \pi/2$ for the first row, while $\tilde{\varphi}_s = 0$ and $\tilde{\varphi}_i = \pi$ in the second row. The pump angular quantum number is $\ell^p = 0$ in figures (a) and (d), $\ell^p = 1$ in figures (b) and (e), and $\ell^p = 2$ in figures (c) and (f). The BBO crystal length is 1mm, its optical axis is located in the Y - Z plane, and the width of the transversal wave number for the Bessel-Gauss photons is $W = 0.0005\mu\text{m}^{-1}$.

propagation invariant can be used to generate heralded single photons with the same property. A detailed study of type I spontaneous down conversion (SPDC) of Bessel-Gauss photons was performed as an interesting example for the study of generation of structured photons from beams that are propagation invariant and also have OAM. Explicit analytical and numerical results were given for the angular and conditional spectrum using a birefringent crystal cut with the optical axis optimized for SPDC with standard Gaussian pump beams. Since the AS and the CAS do not depend on the detailed phase structure of the pump beam in the wave vector domain, the results obtained in this work are expected to be valid for other structured pump beams such as Mathieu and Weber beams.

It was also shown that, as the magnitude of the transverse wave vector of a pump Bessel-Gauss beam increases, the emission cone is deformed into two non coaxial cones which touch each other along a line determined by the orientation of the optical axis of the nonlinear crystal. At this location, the conditional spectrum becomes maximal for a pair of photons, one of which is best described in wave vector space by a Gaussian like photon, with a very small transverse wave vector, and the other Bessel-Gauss photon with the same mean and width distribution of transverse wave vectors as the incident pump photon. Both of them have their main propagation axis close to the cone expected for a Gaussian pump beam. The results were successfully compared with reported experiments. The study on the OAM distribution for the photon pairs showed the existence of clear correlations between the OAM quantum number that can be directly manipulated by varying the pump parameters κ_{\perp}^p and ℓ^p . However, it was also shown that these

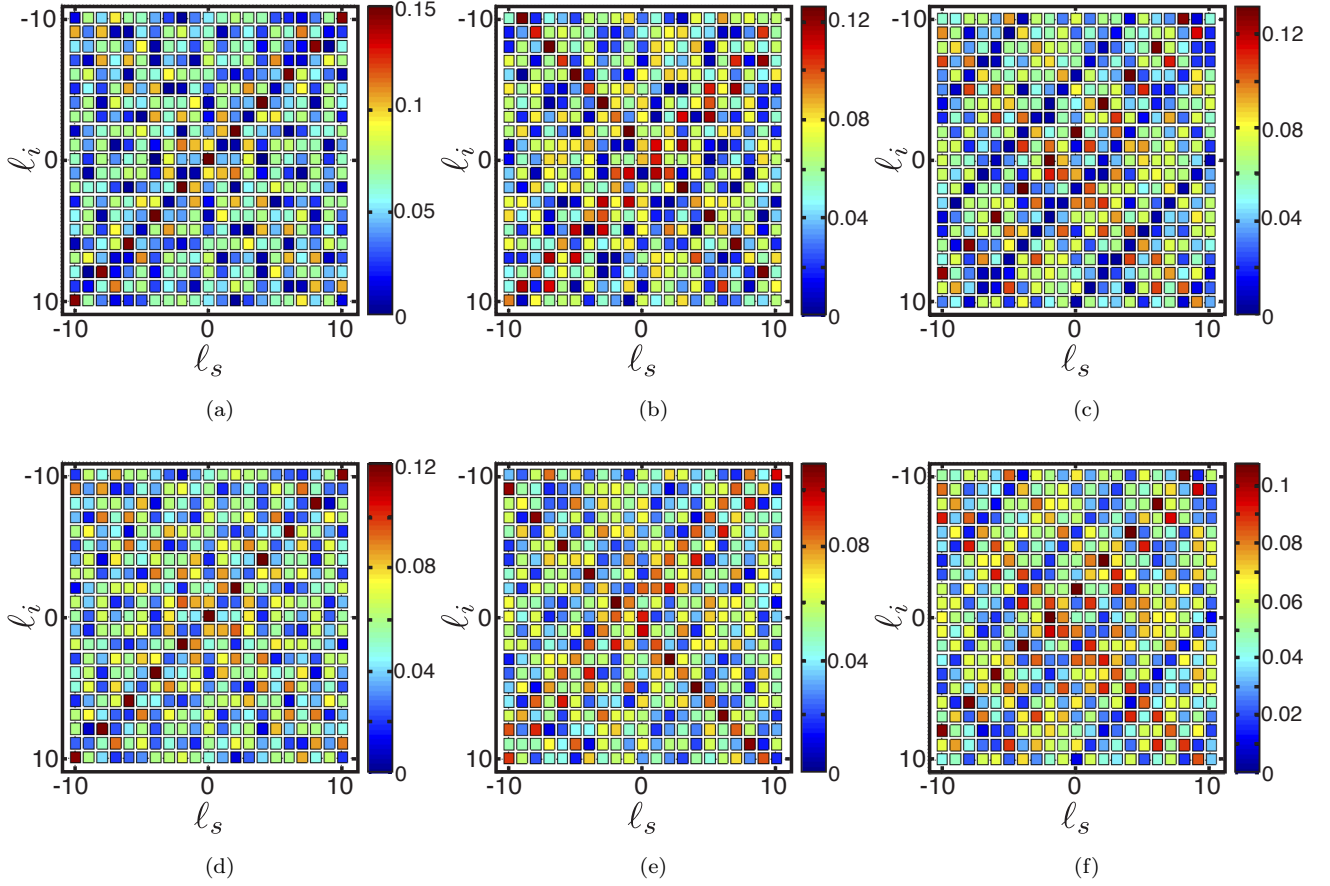


Figure 4: Modulus of the transition element F , Eq. (40), as a function of the orbital angular momentum ℓ^s of the signal and ℓ^i of the idler photon. They involve a pump Bessel Gauss photon with transverse wave number $\kappa_{\perp}^p = 0.05\mu\text{m}^{-1}$, a signal Bessel photon with $\kappa_{\perp}^s = 0.001\mu\text{m}^{-1}$ and an idler photon with $\kappa_{\perp}^i = 0.05\mu\text{m}^{-1}$. The idler and signal photons are emitted with their main propagation axis with orientation angles $\hat{\theta} = \theta_{ec}$ and $\hat{\varphi}_s = -\pi/2$ and $\hat{\varphi}_i = \pi/2$ in the first row, while $\hat{\varphi}_s = 0$ and $\hat{\varphi}_i = \pi$ in the second row. The pump angular quantum number is $\ell^p = 0$ in figures (a) and (d), $\ell^p = 1$ in figures (b) and (e) and $\ell^p = 2$ in figures (c) and (f). The BBO crystal length is 1mm, its optical axis is located in the Y - Z plane and the width of the transversal wave number for the Bessel-Gauss photons is $W = 0.0005\mu\text{m}^{-1}$.

correlations cannot be interpreted in terms of angular momentum conservation.

-
- [1] L. Allen, M. W. Beijersbergen, R. J. C. Spreeuw, and J. P. Woerdman, Phys. Rev. A **45**, 8185 (1992).
 - [2] K. Volke-Sepúlveda, V. Garcés-Chávez, S. Chávez-Cerda, J. Arlt and K. Dholakia, J. Opt. B: Quantum Semiclass. Opt. **S82**, 1464 (2002).
 - [3] C. López-Mariscal, M. A. Bandres, J. C. Gutiérrez-Vega, Opt. Eng. **45**, 068001 (2006).
 - [4] B. M. Rodríguez-Lara and R. Jáuregui, Phys. Rev. A **79**, 055806 (2009); C. L. Hernández-Cedillo, S. Bernon, H. Hattermann, J. Fortágh, R. Jáuregui, Phys. Rev. A **87**, 023404 (2013).
 - [5] G. A. Siviloglou, J. Broky, A. Dogariu, and D. N. Christodoulides, Phys. Rev. Lett. **99**, 213901 (2007).
 - [6] P. G. Kwiat, K. Mattle, H. Weinfurter, A. Zeilinger, A. V. Sergienko, and Y. Shih, Phys. Rev. Lett. **75**, 4337 (1995).
 - [7] H. Bechmann-Pasquinucci and W. Tittel, Phys. Rev. A **61**, 062308 (2000).
 - [8] A. Mair, A. Vaziri, G. Weihs, and A. Zeilinger, Nature **412**, 313 (2001).
 - [9] S. Hacyan and R. Jáuregui, Journal of Optics A: Pure and Applied Optics **11**, 085204 (2009).
 - [10] C. I. Osorio, G. Molina-Terriza, and J. P. Torres, Phys. Rev. A **77**, 015810 (2008).
 - [11] S. P. Walborn, C. H. Monken, S. Pádua and P. H. Souto Ribeiro, Physics Reports **495**, 87 (2010).

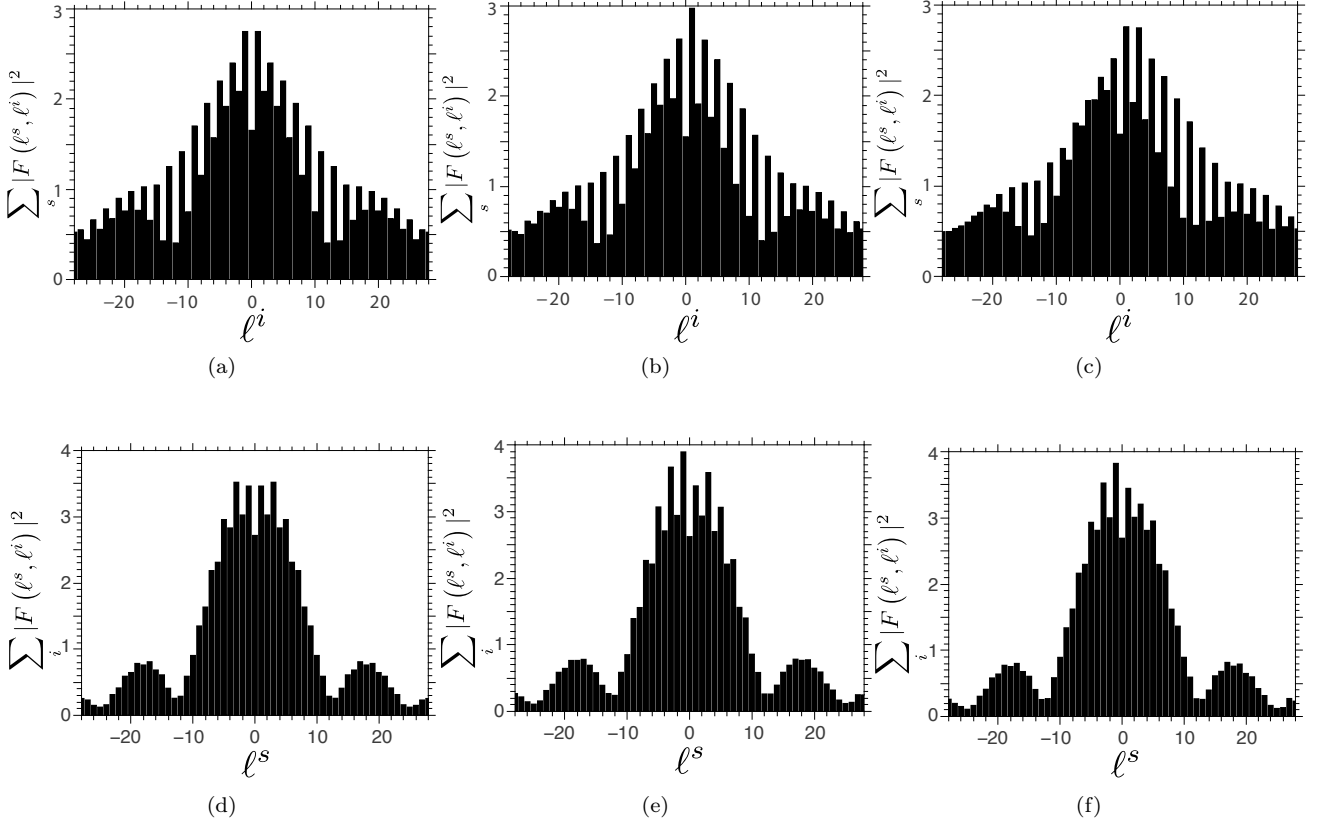


Figure 5: Marginal distribution of orbital angular momentum of the signal ℓ^s and idler ℓ^i photon. They involve a pump Bessel Gauss profile with transverse wave number $\kappa_{\perp}^p = 0.01\mu\text{m}^{-1}$, a signal Bessel photon with $\kappa_{\perp}^s = 0.0001\mu\text{m}^{-1}$ and an idler photon with $\kappa_{\perp}^i = 0.01\mu\text{m}^{-1}$. The idler and signal photons are emitted with their main propagation axis with orientation angles $\tilde{\theta} = \theta_{ec}$ and $\tilde{\varphi}_s = -\pi/2$ and $\tilde{\varphi}_i = \pi/2$. The pump angular quantum number is $\ell^p = 0$ in figures (a) and (d), $\ell^p = 1$ in figures (b) and (e), and $\ell^p = 2$ in figures (c) and (f). The BBO crystal length is 1 mm, its optical axis is located in the Y-Z plane and the width of the transversal wave number for the Bessel-Gauss photons is $W = 0.0005\mu\text{m}^{-1}$.

- [12] M. V. Fedorov, M. A. Efremov, P. A. Volkov, E. V. Moreva, S. S. Straupe, and S. P. Kulik, Phys. Rev. A **77** 032336 (2008).
- [13] A. V. Burlakov, M. V. Chekhova, D. N. Klyshko, S. P. Kulik, A. N. Penin, Y. H. Shih, and D. V. Strekalov, Phys. Rev. A **56**, 3214 (1997); C. H. Monken, P. H. Souto Ribeiro, and S. Pádua, Phys. Rev. A **57**, 3123 (1998).
- [14] H. Cruz-Ramírez, R. Ramírez-Alarcón, F. J. Morelos, P. A. Quinto-Su, J. C. Gutiérrez-Vega, and A. B. U'Ren, Opt. Express **20**, 29761 (2012).
- [15] C. K. Hong and L. Mandel, Phys. Rev. A **31**, 2409 (1985).
- [16] The description of structured light in terms of scalar modes is necessarily approximate. Linear polarized Bessel modes have necessarily a component of the electric field along the main direction of propagation that can be neglected in the paraxial approximation. See, e. g. R. Jáuregui and S. Hacyan, Phys. Rev. A **71**, 033411 (2005).
- [17] That is not the case for Laguerre-Gaussian beams taken as pump beams in SPDC. They are paraxial beams that also carry orbital angular momentum; their angular spectra contains a factor k_{\perp}^{n+2m} that yields a dependence on m of the corresponding joint amplitude.
- [18] Y. Jerónimo-Moreno and R. Jáuregui, submitted for publication.